DOI: 10.1002/ejic.200600161

Artificial Light-Harvesting Systems by Use of Metal Coordination

Yoshiaki Kobuke*[a]

Keywords: Energy conversion / Complementary coordination / Porphyrinoids / Phthalocyanines / Perylenebisimide / Bi(ter)pyridyl complex

Construction of artificial light-harvesting systems by metal coordination is reviewed. Light absorbing dyes include porphyrin, phthalocyanine, perylenebisimide and polypyridyl metal complexes. The supramolecular assemblies are obtained by ligand coordination to metal ions in the center or exterior of the chromophores. Supermolecules of discrete structures even in the solution phase are focused on, and methodologies to acquire large association constants are discussed. Complementary or multitopic coordination to the Zn^{2+} ion gives satisfactory results in obtaining stable and discrete supramolecular structures while maintaining the singlet excited state. Fast energy transfers among the chromophore units are analyzed satisfactorily to examine the properties of light-harvesting antennae. Use of transition-metal ions provides strong coordination, but intersystem crossing of the singlet excited state to the triplet becomes significant. Photophysical properties of such triplet excited species are reported in a limited number of cases and their properties are discussed in view of the light-harvesting antenna function.

1. Introduction

Photosynthetic oxidation-reduction reactions start at the reaction center by ejecting an electron from the photoexcited primary electron donor, the chlorophyll dimer of the so-called special pair or monomeric chlorophyll in more evolved systems to the primary electron acceptor. This reaction center is surrounded by a large number of light-harvesting antenna chlorophylls in order to make the maximum use of the incoming photons. When a photon hits one of the chlorophyll molecules, the excitation energy must be transferred to the far reaction center without losing the energy. There are several decay processes to lose the singlet excited state: intersystem crossing to the corresponding triplet state, emission through fluorescence, and nonemissive internal conversions. Since the lifetime of the singlet excited chlorophylls is generally of the order of nanoseconds, the energy transfer must take place with time constants faster than the order of a nanosecond.

An artificial light-harvesting system is interesting from various viewpoints. Understanding the way that nature per-

[a] Graduate School of Materials Science, Nara Institute of Science and Technology,
8916-5 Takayama, Ikoma, Nara 630-0192, Japan,
Fax: +81-743-72-6119
E-mail: kobuke@ms.naist.jp

Yoshiaki Kobuke obtained his Bachelor degree from the Department of Synthetic Chemistry, Faculty of Engineering in 1964 at Kyoto University, where he worked under the supervision of Prof. Ryohei Oda. He joined the group of Prof. Junji Furukawa at the same Department as a graduate student in 1964. His thesis work for which he received his Ph.D. in Engineering was on the study of mechanisms of stereospecific polymerization and endo-exo stereoselectivities of Diels–Alder reactions. In 1969 he joined the Department of Synthetic Chemistry, Faculty of Engineering at Kyoto University as an Assistant Professor and collaborated with Prof. Junji Furukawa. In the period of 1972–1973 he joined the group of Prof. Robert Burns Woodward as a research associate in the Department of Chemistry at Harvard University for the total syntheses of Vitamin B12 and erythromycin. After the retirement of Prof. Furukawa in 1977, he collaborated with Prof. Iwao Tabushi. In 1980 he was promoted to Associate Professor. In 1990, he was appointed to Professor in the Department of Materials Science, Faculty of Engineering at Shizuoka University. The main research target was the synthesis of artificial ion channels and their characterization by single channel current observations. In 1998 he moved to the Graduate School of Materials Science, Nara Institute of Science and Technology. During 1998–2003 he was a project leader of CREST (Core Research for Evolutionary Science and Technology from the Japan Science and Technology Corporation). His research interest is artificial photosynthesis focusing on its initial events, i.e. antenna function and charge separation. Studies on novel two photon absorbing materials and artificial ion channels are under way.

MICROREVIEWS: This feature introduces the readers to the authors' research through a concise overview of the selected topic. Reference to important work from others in the field is included.

forms intricate functions should be of profound interest. In the case of light-harvesting antenna, visually aesthetic crystallographic structures are already known. Their well-organized structure is thought to correlate closely with the functions they perform. If we succeed in establishing the nature of the structure-function relationship, we will obtain the method by which the photo-excited energy is stored in molecules or molecular systems, and transferred with minimum loss. This knowledge can then be applied not only to the construction of artificial photosynthetic systems and solar energy conversion systems, but also to the development of photonic and electronic materials by the use of chromophores having expanded π-electronic systems.

An artificial light-harvesting system may best be achieved by mimicking the purple bacterial system, since the structure-function relationship may be understood best in the simplest way. Therefore, macrocyclic arrangements of porphyrins and other chromophores will be the first choice. Covalent linking is the most classical and productive method. There are numerous examples reported, and also review articles.[1–5] Alternatively, a supramolecular approach to this target may have special importance, since the natural structure is one of the best examples as will soon be explained. In this article, the author will focus on the supramolecular approach to the construction of a light-harvesting system. As a requisite to clear discussions based on structural information, the species having discrete structures in solution will be treated. In view of strong coordination and definite coordination angle, metal coordination may play the most important role.[6–16]

Nature uses only the singlet excited state for photosynthesis and specially protects against the formation of the triplet state. This does not necessarily mean that the artificial systems should use the singlet excited species. The triplet excited species have longer lifetimes and the $[Ru(bpy)_3]^{2+}$ complex and its derivatives have been successfully used for dye-sensitized solar cells. However, the detailed analysis of the triplet energy transfer processes is accompanied by added difficulties compared with that for the singlet species. Therefore many potential complexes are prepared by using transition-metal ions, without mentioning the photophysical properties. Here, discussion will focus on supermolecules and the measurement of their photophysical properties.

2. Natural Light-Harvesting Systems

In order to achieve effective charge separation, Nature has designed a most sophisticated molecular system for the reaction center. It is not clever to place such a system in all the light-receiving spots so the reaction center is instead accompanied by a large number of light-harvesting devices in the surrounding space. This system resembles a central factory system appropriate for mass production, and is maintained by the supply of light harvesting devices of simple structure for the unitary function.

The arrangement of a bacterial photosynthetic system was first analyzed by X-ray crystallography in 1995.[17–22] The light-harvesting complex LH2 from purple bacteria is composed of B800 and B850. B800 contains nine bacteriochlorophylls arranged in a planar circle form. In contrast, B850 contains 18 bacteriochlorophylls in a barrel form arranged perpendicularly to B800. The light energy absorbed by B800 is transferred to B850 according to the cascading energy transfer. The excitation energy travels further to other B850s and finally reaches LH1. Here, 30 bacteriochlorophylls are arranged in a barrel form similar to B850, except for having one open exit. In addition, LH1 contains the reaction center in the central space. Therefore, the excitation energy reaching LH1 is transferred effectively to the special pair initiating the charge separation. The arrangements of B850, LH1, and interestingly even the special pair are given by coordination of the imidazolyl side chains in transmembrane helices to the central Mg^{2+} ion in the bacteriochlorophyll. The energy transfer rates in the supramolecular arrangements (Figure 1) are as fast as the order of picoseconds within lifetimes of the order of nanoseconds.[23–30]

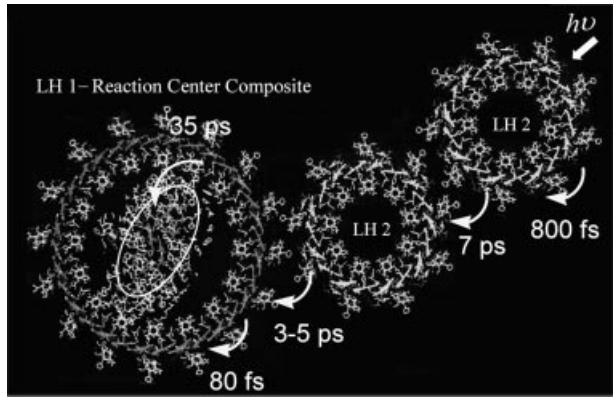

Figure 1. Scheme of light harvesting in photosynthetic purple bacteria.[22]

As seen above, the light-harvesting system of bacteria employs very regular arrangements of bacteriochlorophylls. This is not general for all the light-harvesting antenna systems. Antennae in plants and cyanobacteria, both being very similar, seem to use a totally different architecture.[31–35] Figure 2 shows the crystallographic structure of cyanobacterial photosystem I as a trimer, which represents the existing form also in vivo. The monomer contains a large number of chromophores of 90 chlorophyll *a* molecules and 22 carotenoids. This is a core antenna system and is accompanied further by separately existing antenna components, which are normally associated with photosystem II. It must be noted that a plant employs almost the same architecture as cyanobacteria. It is remarkable that the system employed by cyanobacteria 2.5 billion years ago is still effective even 1 billion years after plants first evolved. Almost no evolutional change of the structure may signify that the perfect form of the antenna system has been arrived at. However, it seems extremely difficult to extract a simple constitutional principle from the apparently random architecture.

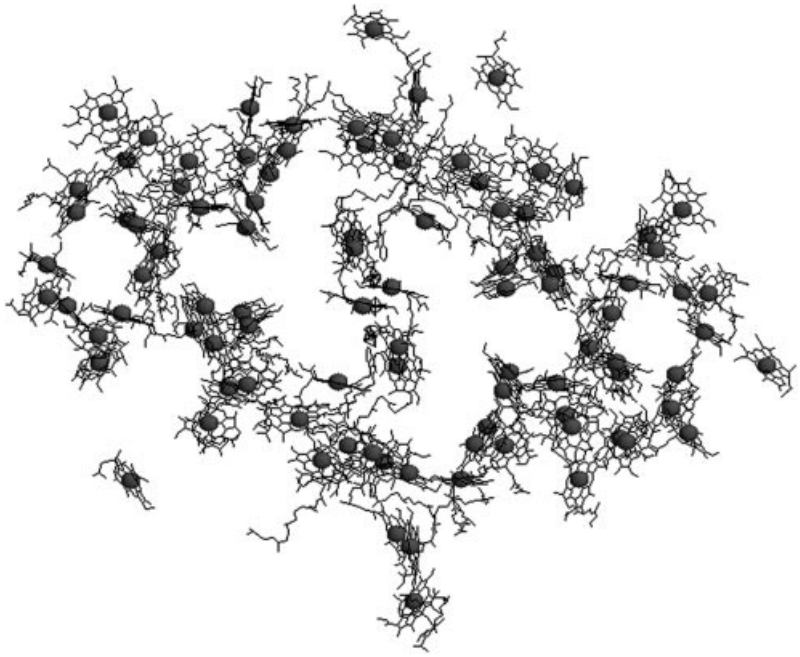

Figure 2. Crystal structure of cyanobacterial photosystem I. Prepared from Brookhaven Data Bank file 1JB0.[31]

3. Chromophores

In light-harvesting devices, incoming light energy must be captured efficiently by one of the chromophores distributed widely in the surrounding space and transferred efficiently to the reaction center. For this purpose, nature employs chlorophyll-*a* and -*b* or the corresponding bacteriochlorophylls as the light-absorbing unit. They have extinction coefficients as large as 10^5–10^6 cm^{-1} M^{-1} near the regions at 400 and 600 nm. Chromophores closely related to chlorophyll derivatives are porphyrin and phthalocyanine. Recently, the use of perylenebisimide has been demonstrated to be excellent for such purposes. Ruthenium tris-bipyridine or bis-terpyridine have unique characteristics for such purposes and are widely used for photocurrent generation systems. The typical characteristics of these chromophores are compared in Table 1. Figure 3 shows the absorption spectra at the same extinction coefficient scale for easy comparison of their relative magnitudes.

The photosynthetic reaction is conducted through the singlet excited state and its conversion to the triplet is strictly protected by several mechanisms. It is important to

Table 1. Photochemical characteristics of typical chromophores used for natural and artificial antenna systems.

Compounds[a]	Fluorescence quantum yield	Fluorescence lifetime [ns]	Phosphorescence quantum yield	Phosphorescence lifetime [μs]	Ref.
Chl *a*	0.3	6.1			[36]
Chl *b*	0.117				[37]
BChl *a*	0.18	3.1			[38]
BChl *c* (monomer)	0.29	6.5			[38]
BChl *c* (aggregate)	0.5	3.3			[38]
H_2TPP	0.13	6.3	0.87		[39]
ZnTPP	0.033	1.92			[40]
MgTPP	0.15	9	0.8		[41,42]
H_2Pc	0.6	5.5		0.28[b]	[43,44]
ZnPc	0.3	3	0.1[b]	1100[b]	[43]
MgPc	0.84	5.7	$5\cdot10^{-6}$[b]	1000[b]	[45]
Perylenebisimide, $(OAr)_4$	0.92	6.1			[46]
$[Ru(bpy)_3]^{2+}$			0.042	0.63	[47]
$[Ru(tpy)_2]^{2+}$			$<5\cdot10^{-6}$	–	[48]
$[Ru(4'\text{-Phtpy})_2]^{2+}$			$4\cdot10^{-5}$	0.001	[48]
$[Ru(4'\text{-Cltpy})_2]^{2+}$			$<1\cdot10^{-5}$	0.0002	[48]

[a] Chl = chlorophyll, BChl = bacteriochlorophyll, H_2TPP = tetraphenylporphyrin, ZnTPP = zinc tetraphenylporphyrin, MgTPP = magnesium tetraphenylporphyrin, H_2Pc = phthalocyanine, ZnPc = zincphthalocyanine, MgPc = magnesiumphthalocyanine, perylenebisimide = 1,6,7,12-tetraarylperylenebisimide, $[Ru(bpy)_3]^{2+}$ = [ruthenium tris(bipyridine)]$^{2+}$, $[Ru(tpy)_2]^{2+}$ = [ruthenium bis(terpyridine)]$^{2+}$, $[Ru(4'\text{-Phtpy})_2]^{2+}$ = [ruthenium bis(4′-phenylterpyridine)]$^{2+}$, $[Ru(4'\text{-Cltpy})_2]^{2+}$ = [ruthenium bis(4′-chloroterpyridine)]$^{2+}$. [b] From ref.[49] (77 K).

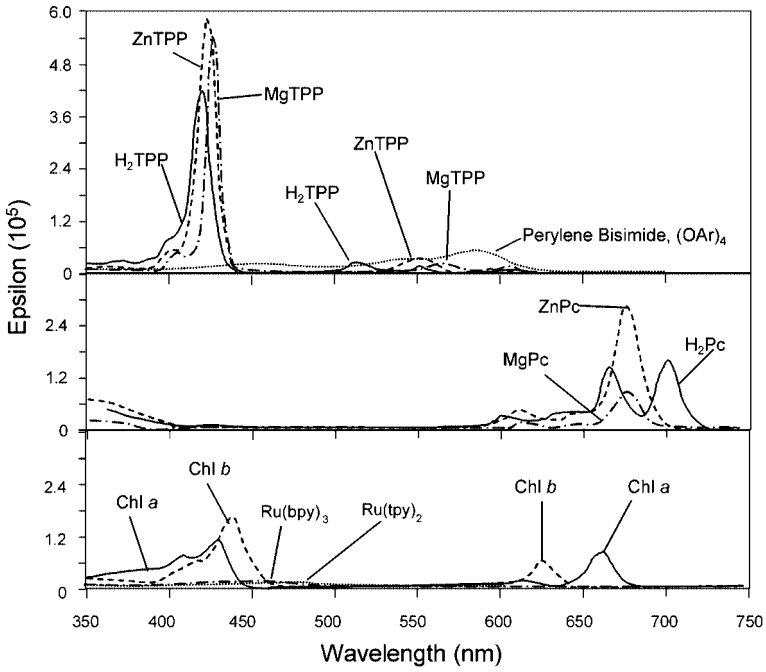

Figure 3. Comparison of absorption spectra of chromophores in Table 1 at the same scale of extinction coefficient, with the same codes as used in Table 1.[46,48,50]

transfer the singlet excitation energy within the lifetime. Therefore, close inter-chromophore distances are critical to ensure the successful fast excitation energy transfers, as observed for the B850 and LH1 systems. The close interchromophoric distance induces strong exciton interaction as shown schematically in Figure 4. Face-to-face interaction induces a blue shift of the absorption wavelength, while head-to-tail interaction shifts the absorption band to a longer wavelength.[51] The excited state of the face-to-face interaction tends to lose its excitation energy through internal conversion to the vibrational energy and decay without fluorescence emission. On the other hand, excitons with a head-to-tail orientation can maintain the excited state and transfer the excitation energy within the lifetime. By using the red shift of the absorption wavelength, a vectorial energy transfer pathway can be constructed.

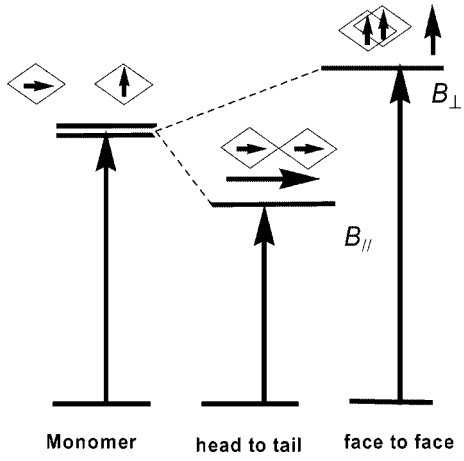

Figure 4. Exciton interaction of transition dipoles.[51]

4. Methods of Coordination Assembly

The assembly formation sometimes induces the formation of an energy sink, where the singlet excitation energy is lost through internal conversion to vibrational states. Random assembly of chromophores induces this kind of unfavorable defect formation, and for this reason regular arrangement of the chromophores is desirable. There are several methods to assemble chromophores through supramolecular assembling.

Coordination to metal ions provides the strongest intermolecular forces among others such as hydrogen bonds, ionic interactions, and π-π stacking interactions. It is important to obtain chromophore assemblies of discrete structure for the discussion based on a clear molecular basis. From this viewpoint, metal coordination provides the best intermolecular force for chromophore assembly. Other intermolecular forces are also used in combination with metal coordination, but are hardly expected to obtain supermolecules of discrete structure in solution by using their weak intermolecular forces alone.[52,53]

The nature of metal ions has a large effect on the characteristics of the resulting metal-coordinated chromophore assemblies. Metal ions of typical groups and d^{10} transition-metal ions do not have much influence on the singlet excited state. However, transition-metal ions having odd electron spins tend to quench the singlet excitation energy through interaction with their odd spin. Therefore, the use of paramagnetic transition-metal ions for the assembly formation must be primarily avoided. The former class of metal ions, however, in general provides only a weak ligand field with small stability constants and allows equilibrium with free ligands. Assemblies have been obtained with due consider-

ation of the above characteristics and limitations. The modes of complexation will be classified into two types as illustrated in Figure 5.

Type I: Coordination of the chromophore's ligand to metallochromophore.

Type II: Coordination of the chromophore's ligand to external metal ions.

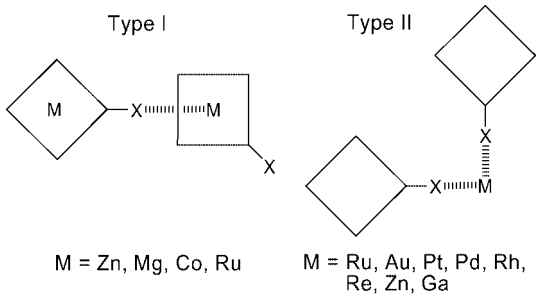

Figure 5. Mode of assembly formation by coordination, with the square and X representing chromophore and coordinating ligand, respectively.

As chromophores containing metal ions, porphyrin and phthalocyanine provide the most typical examples for Type I assembly formation. Chlorophyll employs Mg^{2+} but artificial systems use Zn^{2+} as the most typical substitute, since Zn^{2+} has a d^{10} electronic configuration without odd spin. Zn^{2+} complexes are practically stable toward heat, acidic condition, and oxidation. The artificial system prefers Zn^{2+} in most cases based on these properties, although its fluorescence quantum yield is inferior to Mg^{2+} systems. Since Zn^{2+} cannot provide a strong ligand field, the stability constant is not inherently very large, unless multitopic or complementary coordination is designed. Unique ideas have therefore been developed for obtaining stable assemblies.

When transition-metal ions are incorporated into the central core of porphyrins and phthalocyanines, even mono-axial coordination can afford large stability constants. However, the intersystem crossing of singlet to the triplet states occurs and light harvesting through the triplet pathway must become the main route.

When the assembly inducing metal ion locates outside the chromophore, the flexibility of the molecular design for assembly formation increases. Chelation may be powerful for obtaining stable complexes. Nanoparticles developed recently may also be interesting.

5. Porphyrin with an Inner-Ring Metal Ion

Central metals accommodated in the macrocyclic structure allow one or two axial coordinations of ligand depending on the metal ion species. Penta-coordinating Zn^{2+} accepts only one axial coordination. Neutral nitrogen ligands generally afford large stability constants, but simple monocoordination is not strong enough to maintain the discrete structure under μM concentrations for which special molecular designs are required. Kobuke proposed the idea of complementary coordination of an imidazolyl substituent of one porphyrin to the Zn^{2+} center of another porphyrin, whose imidazolyl coordinated back to Zn^{2+} in the original porphyrin.[54,55] The stability constant reaches 10^{11} M^{-1} in nonpolar solvents. The factor that contributes most to such a large stability constant is the complementarity of the imidazolyl–Zn–porphyrin. Compared with other potential ligands such as pyridyl, imidazolyl has the following advantages (see Figure 6):

(1) High basicity leading to high coordination ability.

(2) Smaller angle strain from the ideal (vertical to the macrocyclic plane) coordination angle.

(3) Smaller steric hindrance from substituents at positions α to the ligating N atom.

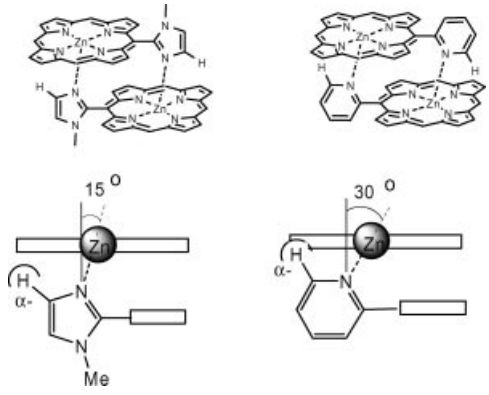

Figure 6. Complementary coordination of imidazolyl and pyridyl to Zn^{2+}, where the rectangle denotes porphyrin.

This motif can be applied to the formation of linear and macrocyclic species, both of which are regarded as excellent light harvesting antennae. Firstly, in order to obtain linear porphyrin arrays based on complementary coordination, two imidazolyl–Zn–porphyrin units were connected directly at their *meso* positions, as shown in compound **1**. Since the coordination grows to both sides opposite to each other, the successive complementary coordination leads to a linear multi-porphyrin array **2** (Figure 7A).[56] The molecular weight was extremely high reflecting the large stability constant of the complementary coordination and the number of the longest porphyrin unit reached 800 porphyrin units with a distribution peak of 160 units. However, the coordination bond is cleaved and regenerated by adding and eliminating coordinating solvents, respectively. An example was shown by GPC elution curves (A) and (B) in part B of Figure 7. A mixture of *meso*-*meso*-linked bisporphyrin **1** and monoimidazolylporphyrin **3** showed the corresponding two peaks in $CHCl_3$ (A). When methanol was added to the chloroform solution, followed by evaporation to cleave and regenerate the coordination, bisporphyrin oligomers terminated by monomeric porphyrins **4** were obtained (B).

It is noteworthy that this linear assembly does not induce fluorescence quenching. Evaluation of the energy transfer rate along the one-dimensional array is not as easy as in the degenerated array of the ring. Therefore, fluorescence-quenching Mn–porphyrins were attached at both the terminals of the linear array by using hetero-complementary coordination of imidazolyl–Mn–porphyrin **5** to the terminal

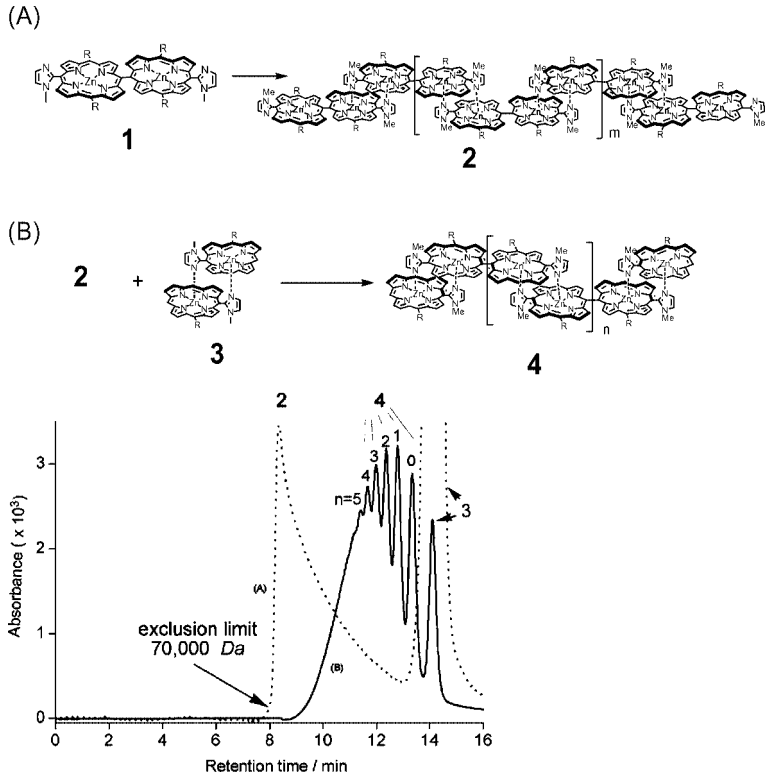

Figure 7. (A) Linear array formation of bis(imidazolylzincporphyrin) and (B) linear array with terminal monoimidazolylporphyrins and its GPC characterization.[56]

imidazolyl–Zn–porphyrin (Figure 8).[57] It is possible to design the array **6** of 200 Zn-porphyrin arrays terminated by Zn–Mn hetero-coordination by considering the relative strength of hetero Mn–Zn and homo Zn–Zn and Mn–Mn complementary coordinations. Under such conditions, photoexcitation of any porphyrin in the terminal 130 arrays leads to quenching by the terminal Mn–porphyrins, suggesting that rapid and efficient energy transfer is occurring along the linear array.

The linear porphyrin arrays are characterized by two important properties: no fluorescence quenching on array formation and efficient energy transfer along the array. Photocurrent generation by use of a dye-modified flat electrode may provide interesting applications for fields other than the conventional surface-coated porous semiconductor materials. In the former case, the efficient light-harvesting system becomes critical to compensate for the decreased surface area. Imidazolyl–Zn–porphyrin appended with an ω-mercaptoalkyl group is employed as a key element connecting the Au electrode surface and the porphyrin arrays.[58,59] Porphyrin appended with thiol **7** can modify the Au surface simply by a dipping process and an imidazolyl–Zn–porphyrin array can grow by a simple immersion procedure into a solution of *meso*-*meso*-coupled imidazolyl-zinc-porphyrin dimer **8**. After rinsing, the complementary coordination pair can be immobilized by covalent linking of *meso*-allyl ether substituents by a ring-closing metathesis reaction.[60,61] This series of procedures can be repeated until multi-porphyrin layers **9** are accumulated as detected by the gradual increase in the characteristic porphyrin absorption

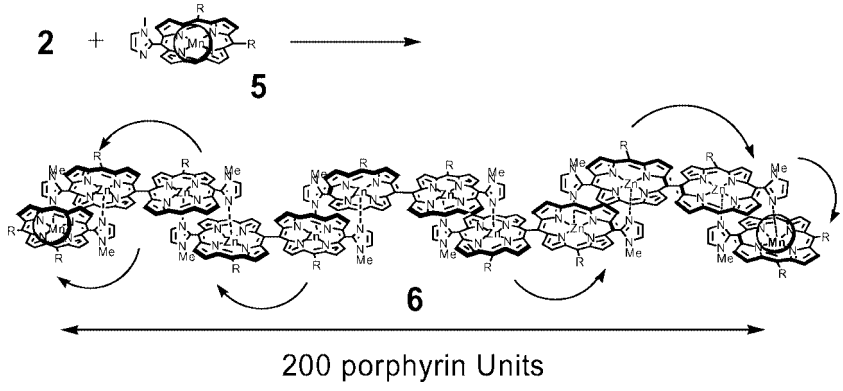

Figure 8. Hetero linear array formation from Zn and Mn porphyrins.[57]

(Figure 9).[62] Light-induced cathodic current was increased as a function of the accumulated amount of the porphyrin, suggesting the light harvesting effect.

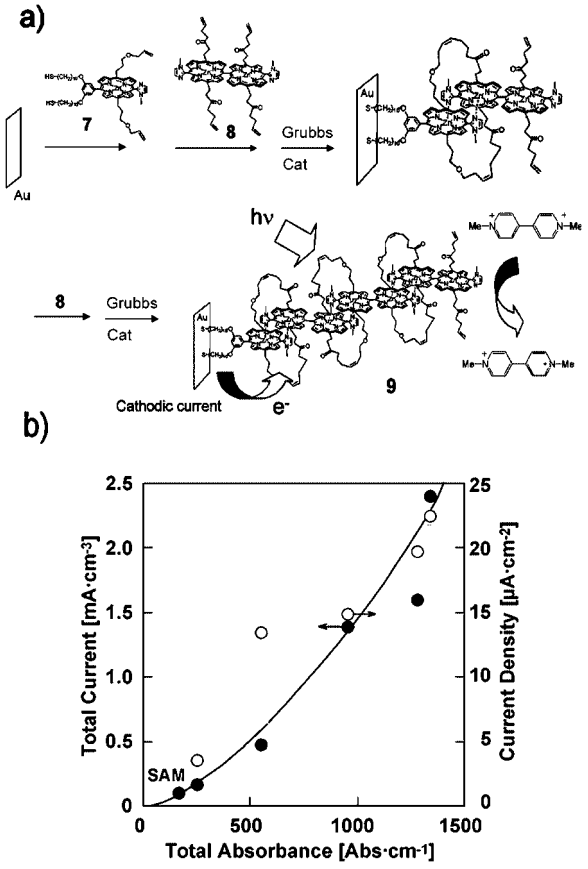

Figure 9. (a) Multiporphyrin array formation on a Au surface and metathesis linking. (b) Dependence of photocurrent on surface grafting.[62]

Two imidazolyl-zinc-porphyrins were then connected through a *m*-phenylene group to adjust the dihedral angle between two porphyrins to 120°, so that bifunctional bis-(imidazolyl–Zn–porphyrin) **10** may be organized into macrocycles, most optimistically to a strain-free hexamer (Figure 10).[63,64] The results were not so simple, but the newly developed reorganization procedure opened up a path to interesting supramolecular methodology leading selectively to macrocyclization. Here, the dynamic nature of imidazolyl-to-zinc coordination plays a critical role. Coordination under normal concentrations (>mM) leads to oligomerization rather than macrocyclization, since the latter process is entropically unfavorable. Then the mixture **11** is first subjected to equilibrium conditions by the addition of coordinating additives, usually MeOH, under high dilution. The successive solvent evaporation leads almost quantitatively to a mixture of macrocycles. The hexamer **12** was accompanied by an equal amount of pentamer **13**, suggesting that the balance of enthalpy and entropy governs the product distribution. Enthalpically, there is no choice of pentamer formation, since it leads to angular strain from the ideal 120°. Entropically a smaller ring is favored, since the encountering probability of two terminal imidazolyl–Zn–porphyrins becomes smaller for a larger ring. In the case of the *m*-phenylene-bridged bisporphyrin, the competition seems equally high for pentamer and hexamer, but far less so for tetramer and heptamer.

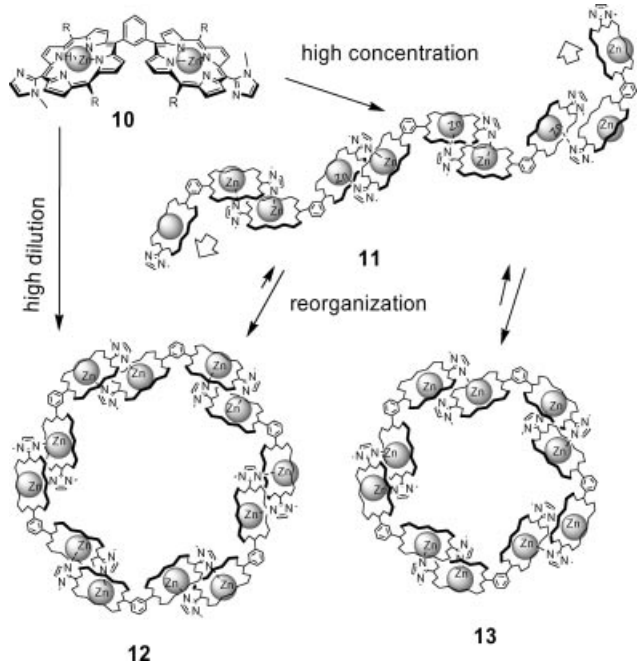

Figure 10. *m*-Phenylene-connected bis(imidazolyl)zincporphyrin and coordination organization.[63]

The assembled macrocycles never lose the fluorescence properties and maintain almost the same quantum yield and lifetime in their fluorescence emission. The energy hopping time constants through the coordination dimer units were determined by the analysis of anisotropy depolarization of the transient absorption spectra after polarized light excitation.[65] At the same time, exciton-exciton annihilation rates were obtained from pump-power dependence on the transient absorption. The coincident time constants from two methods were 8.3 and 5.3 ps for the pentamer and hexamer, respectively (Figure 11). The size-dependent rate constants may represent the effect of orientation factors. Considering the fluorescence lifetime of 2.2 ns, rapid energy transfer should take place 300–400 times during its excited state lifetime. These combined properties prove the excellent light-harvesting antenna models of the B850 type not only in their structure, but also in their function.

When three porphyrins are connected through *m*-phenylene groups and imidazolyls are appended at molecular terminals as in **14**, the self-complementary coordination results in a macrocyclic trimer **15** with a high selectivity under similar reorganization conditions. In this case, the competitive formation of dimer or tetramer is hardly observed because of two unfavorable strain energies. It is interesting that this macrocyclic trimer, which contains three coordination-free zinc-porphyrins, can accommodate tripodal ligand **16** in its hole by multitopic and cooperative coordination (Figure 12).[66] Then, UV and fluorescence titration of this macrocycle with tetrapyridyl ligand **17** in toluene suggested

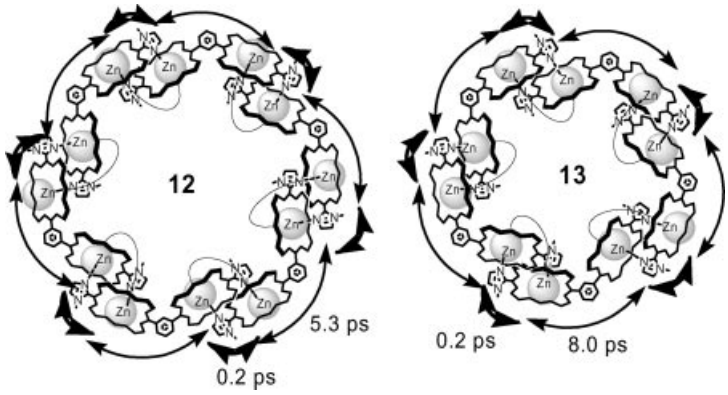

Figure 11. Macrocyclic hexamer and pentamer with excited energy hopping times. The metathesized links in the rear positions are abbreviated.[65]

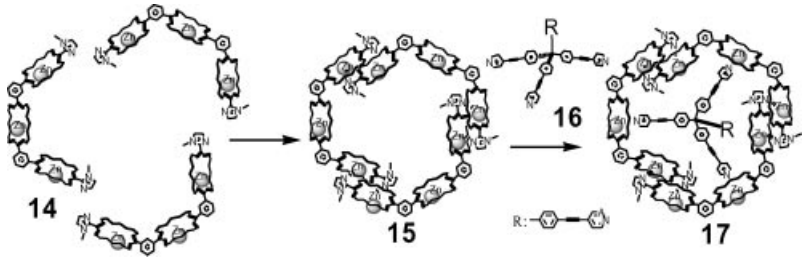

Figure 12. Macrocyclic trimer of trisporphyrin accommodating a tripodal pyridyl ligand.[66]

a stable 1:1 complex with a stability constant of $8 \cdot 10^8$ M^{-1}. When an electron acceptor is appropriately substituted at the fourth arm, the macrocycle can be regarded as a model of an LH1-type antenna.

4-Pyrazolylporphyrin instead of 2-(1-methylimidazolyl)-porphyrin can afford the cyclic trimer according to its angular requirement for coordination.[67,68] The trimer formation is somewhat cooperative, but its stability constant is estimated to be $9.0 \cdot 10^8$ M^{-2} in dichloromethane at 22 °C. In accord with this stability constant, NMR and UV spectra of the trimer species are temperature and concentration dependent in the μM–mM concentration range.

Introduction of an ester group at the *ortho*-position of *para*-phenyl substituent increases the stability constant up to $6.0 \cdot 10^{13}$ M^{-2} through the contribution of additional hydrogen bonding. These trimers have shown similar fluorescence quantum yields and lifetimes to the starting monomeric porphyrin, suggesting no significant perturbation in their S_1 states despite the strong interaction in the S_2 states.

Placement of a nitrogen atom at the 3-position in *meso*-pyridyl derivatives such as the 3-pyridyl or 5-(2-aminopyrimidyl) substituent results in the macrocyclic structure to satisfy the angular dependency.[69,70] The crystal structure suggests the macrocyclic tetramer **18** and **19** as shown in Figure 13, while the structure in solution shows a dynamic equilibrium between the cyclotetramer and other forms depending on other *meso*-substituents, as well as concentration and temperature. Thermochromic change is associated with complexation/decomplexation dynamics in solution at the concentration ca. $1 \cdot 10^{-4}$ M.

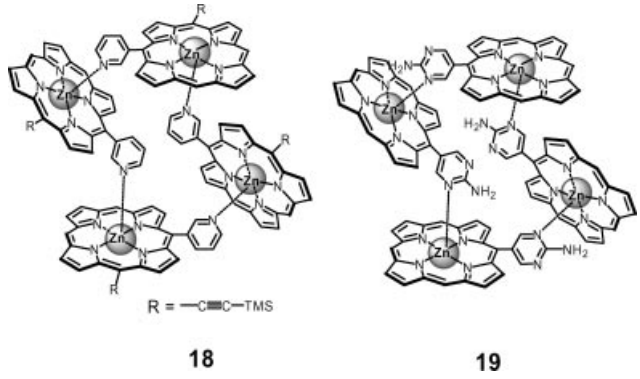

Figure 13. Cyclic tetramer formation from *m*-pyridyl- and pyrimidylzincporphyrins.[69,70]

The control of coordination angle is important for performing the desired cooperativity. The 2,6-dicarbamoylpyridine unit has internal hydrogen bonds to adopt a conformation that orients two arms approximately perpendicular to one another. A rectangular macrocycle **20** using a complementary coordination of the pyridyl unit to zincporphyrin was obtained (Figure 14). The stability constant was evaluated in $CHCl_3$ as $2 \cdot 10^8$ M^{-1}, from which the effective molarity was calculated as 6 M on the basis of the intrinsic binding constant for zinc-pyridine interaction.[71]

Two zincporphyrin units were connected by using this angle-constraining 2,6-dicarbamoylpyridine unit, **21**. Then tetrapyridyl free-base porphyrin **22**, in which intramolecular hydrogen bonds constrain the rotation of the pyridyl li-

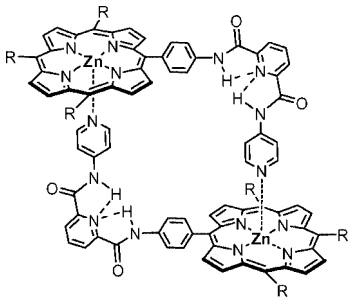

20

Figure 14. Adjustment of coordination angle by hydrogen bonding.[71]

gands, assembled two units of the zincporphyrin by multitopic coordination into a 2:1 mixture of **21** and **22** (Figure 15).[72] The multitopic coordination interaction afforded the stability constant of $2.0 \pm 0.5 \times 10^6$ M^{-1} for each binding event. The overall arrangement constructed a photosynthetic model containing four zincporphyrin units around the free-base porphyrin. The fluorescence intensity of the 2:1 complex **23** showed biphasic decay with a faster component of 490 ps along with a 1330-ps component of the **21**. The energy transfer occurred from **21** to **22** with the rate constant of $2 \cdot 10^9$ s^{-1} and with a quantum yield of 73%. There are several examples of multitopic coordination of pyridyl-appended porphyrins to antenna macrocycles according to covalent approaches.[73–75]

A three-dimensional (3D) box formation is produced by cooperative coordinations. When two porphyrins are connected at the *meso* position, orthogonal conformation is favored by steric repulsion. When 5-(*p*-pyridyl)porphyrin is coupled at the 1-*meso* position, the product becomes a chiral mixture. The mixture is organized by self-coordination to a chiral mixture of three-dimensional bisporphyrin tetramers through homochiral self-sorting processes. The 3D box is favored by its rigidity and is more stable than the monocyclic tetramer from monopyridylporphyrin.[76,77] ω-Pyridyl(phenylene)$_n$-appended zincporphyrins gave similar porphyrin boxes. The energy hopping rates among the unit porphyrins for these box-type assemblies were analyzed by time-resolved spectroscopic methods in conjunction with polarization anisotropy measurements. The data were analyzed by assuming an exciton coherence length of L = 2 for the *meso*-*meso*-coupled dimer. The time constant was explained by a Förster-type incoherent energy hopping model. Therefore, the excitation energy hopping times between the dimeric zincporphyrin units were 48, 98, and 361 ps for **24a**, **24b**, and **24c**, respectively, showing exciton-exciton distance dependence by the bridging (phenylene)$_n$ units (Figure 16).[78]

When porphyrins are connected through a mono- or bisalkynylene unit, two porphyrins prefer to adopt a planar conformation due to a beneficial π-conjugation effect despite the rotational freedom around the triple bond. The zinc complex of bisporphyrin with *meso*-pyridyl functionalities, **25**, self-assembles by coordination to a box-shaped cyclic tetramer **26**, where two conformers, perpendicular and planar, are allowed (Figure 17).[79] In the case of the monoalkynylene-bridge, a planar conformer was the exclusive product reflecting the conformational preference at the monomer level. In the case of the bisalkynylene-bridge, on the contrary, the perpendicular conformer becomes predominant probably because of effective cancellation of the dipole moment, which is induced by the directions of the pyridyl groups in the tetramer.

As discussed earlier, the use of transition-metal ions in the porphyrin metal center cannot be the method of singlet energy harvesting. Although many studies on the structure formation are reported, photophysical studies on the triplet states are rare due to the inherent difficulty of the studies. The following few reports identify the decay processes after the excitation.

Scandola reported on the photophysical behavior of the system of a pentad porphyrin arising from coordination of tetra-*m*-pyridylporphyrin to four Ru(CO)TPP units (**27**)

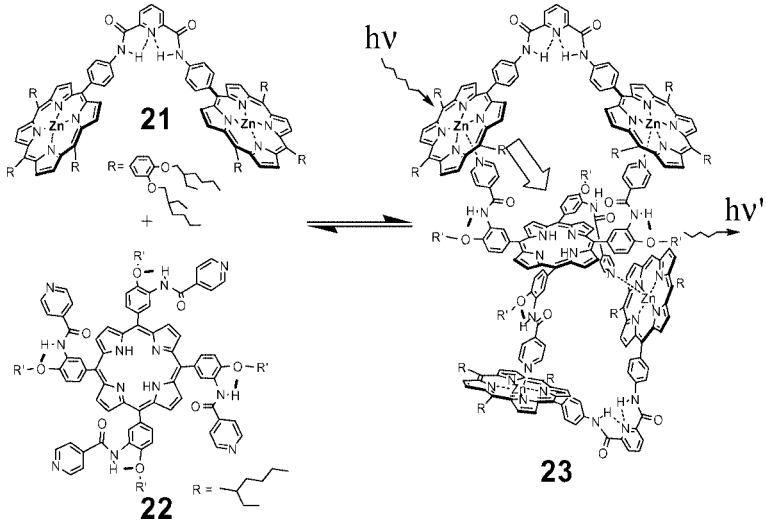

Figure 15. Complementary 2:1 complexation of zinc- and free base porphyrins and internal energy transfer.[72]

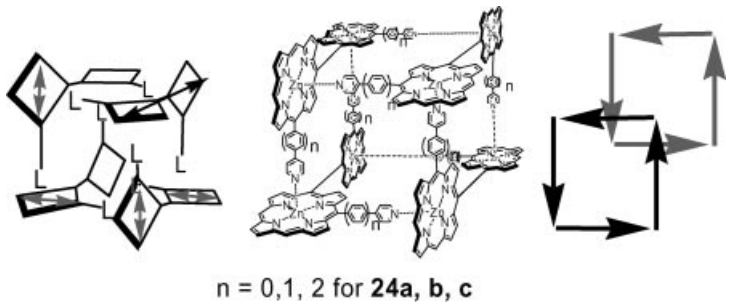

Figure 16. Box formation from *meso-meso* coupled bisporphyrin appended with pyridyl ligand and exciton energy transfer in the box assembly.[77,78]

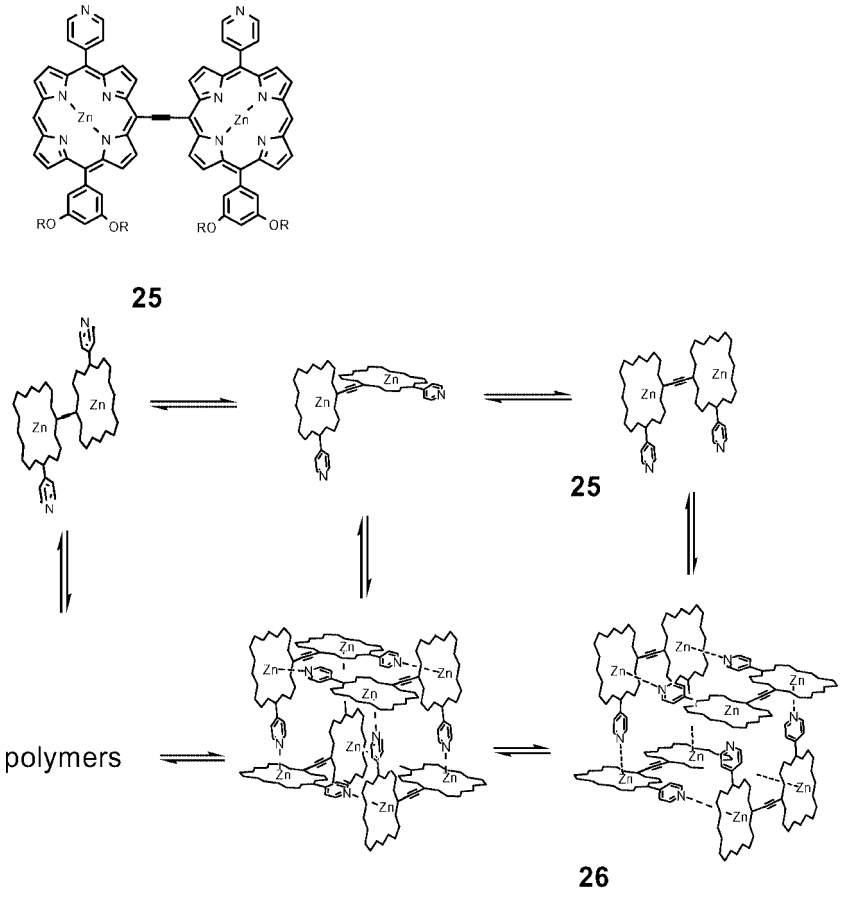

Figure 17. Acetylene-linked bis(pyridylporphyrin) and its coordination organization.[79]

(Figure 18).[80] The lifetime of the free-base porphyrin is shortened significantly to 0.5 ns from around 9 ns for TPP because of the efficient (95%) Ru-facilitated intersystem crossing to ^{3}*Fb by spin-orbit perturbation. Excitation of the Ru porphyrin part leads also to ^{3}*Ru with a much faster time constant (<30 ps) with 100% efficiency, then followed by irreversible energy transfer to ^{3}*FbRu again with 100% efficiency due to the large driving force from Fb^3*Ru to ^{3}*FbRu. The triplet energy transfer rate was estimated to be in the range 10^8–10^9 s^{-1}. When zinc porphyrin is used as the axial ligating unit, the higher energy level of ^{3}*Zn makes the energy difference between ^{3}*ZnRu and Zn^3*Ru smaller and the equilibrium between two triplet states is established prior to deactivation.

Ruthenium porphyrin was connected by another chromophore, pyridyl-substituted perylenebisimide to afford a side-to-face supramolecular array of chromophores (**28**).[81] The absorption spectrum covers the full range of 350–620 nm with an extinction coefficient larger than 10^4 M^{-1} cm^{-1}. The photophysical properties obtained by using nano- and femtosecond time-resolved techniques are summarized in Figure 19. When the perylenebisimide (PBI) part (585 nm) is irradiated, the characteristic strong fluorescence (λ_{max} = 620 nm) of the parent PBI is completely

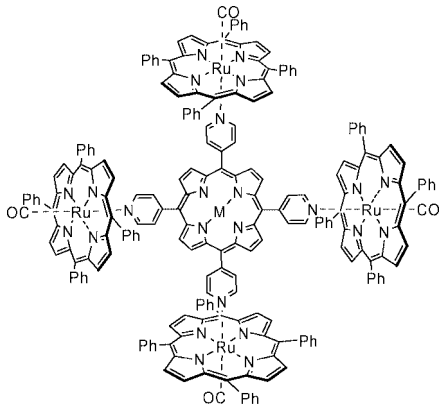

27 M = H_2, Zn

Figure 18. Axial coordination of tetrakis(pyridyl)porphyrin to four Ru^{2+}(CO)porphyrins.[80]

quenched (Φ = 0.001), compared with Φ = 0.96 for free PBI. The spectral change was characterized by the rise of the typical absorption band of the radical anion of PBI near 780 nm, associated with the formation of the Ru(TPP)CO radical cation. The change, with a time constant of 5.6 ps, clearly shows electron transfer from Ru(TPP)CO to ^{1}*PBI. Excitation of the Ru(TPP)CO part (530 nm, although accompanied with PBI excitation), on the other hand, leads to the formation of ^{3}*Ru(TPP)CO by fast intersystem crossing within 1 ps. Then energy transfer occurs from ^{3}*Ru to PBI to generate a new species of ^{3}*PBI. The triplet species of ^{3}*PBI with a lifetime of 9.8 μs in deaerated CH_2Cl_2 is therefore obtainable by the irradiation of the Soret band region of the Ru(TPP)CO site.

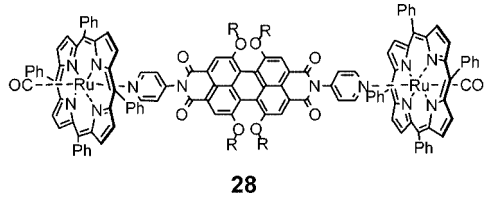

28

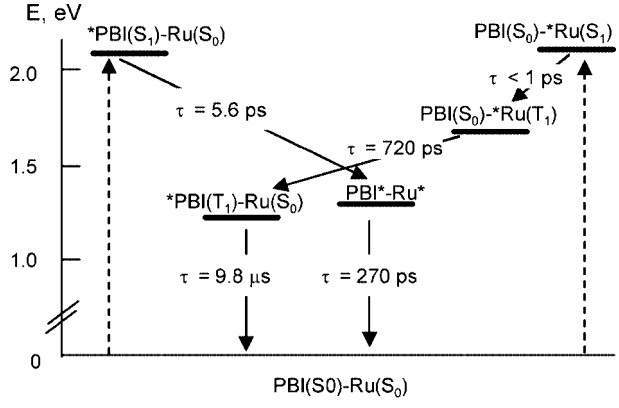

Figure 19. Formation of perylenebisimide-Ru^{2+}porphyrin and photophysical pathways.[81]

6. Porphyrin with an Outer-Ring Metal Ion

The use of transition-metal ions from external sources is a powerful tool for obtaining various self-assemblies and has been well documented. Fujita and Ogura introduced first an elegant way of coordination organization, in which the combination of *cis*-coordination transition-metal ions and linear bridging ligands gave the most thermodynamically stable macrocycles after equilibrium.[82–85] When a porphyrin is employed as the component of the linear bridging ligand, macrocycles composed of porphyrin units are easily obtained. Alessio has already addressed these examples focusing on this methodology in his review.[11] However, the resulting assembly in most cases loses its fluorescence and photophysical studies through phosphorescence emission are rather limited.

Scandola examined the effect of external Ru complexes, which connect pyridyl-porphyrins, on the quenching of the porphyrin singlet. It was found that two mechanisms are operative in the adducts and that their contributions are dependent on the type of Ru complex. One is an enhanced intersystem crossing from Por(S_1) to Por(T_1) by interaction with centers of Type I Ru complexes (Figure 20).[86] The singlet quenching is proportional to the number of Ru centers. The other mechanism is singlet-triplet energy transfer from Por(S_1) to Ru(T_1) of the centers of Type II Ru complexes and provides an additional channel. The latter contribution depends on the energy level of the Ru(T_1) state in the coordination environment at the Ru center. The energy levels of Ru(T_1) with weak field ligands, such as DMSO, are low compared with the ones with strong field ligands, such as CO. The fluorescence lifetimes of the compounds **29**–**31** are reasonably explained by these mechanisms.

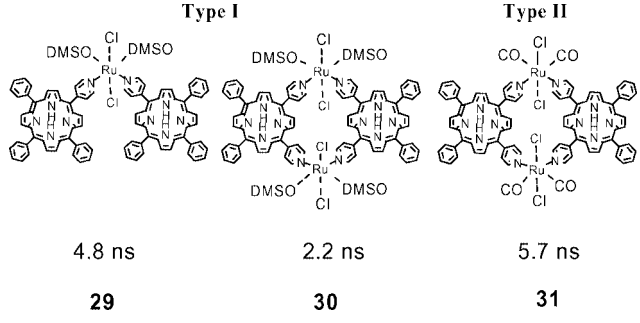

Figure 20. Organization of porphyrin by using external Ru^{2+} coordination.[86]

The square porphyrin nonamer **33** is formed in solution by the addition of *trans*-coordinating bis(benzonitrile)Pd^{2+} dichloride to a stoichiometric mixture of one central X-shaped unit (porphyrin **32a**), four T-shaped units (porphyrin **32b**), and four L-shaped units (porphyrin **32c**) (Figure 21).[87,88] The fluorescence emission of the solution mixture is quenched to greater than 90%. In accord with this observation, the fluorescence lifetime is shortened from 12 ns (the average lifetime for the initial mixture) to less than 1 ns. The claim of a light-harvesting effect must await analysis of how the triplet excited state behaves.

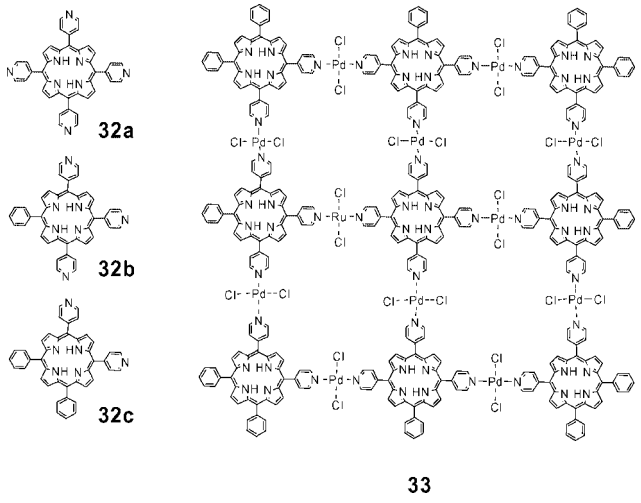

Figure 21. 2D porphyrin array by using *trans*-Pd^{2+} complex.[87]

Rhenium tetramers of free-base and Zn^{2+} porphyrins **34a** and **34b** may be a rare example of fluorescent metallamacrocycles (Figure 22).[89] Into this host cavity, tetrakis(4-pyridyl)porphyrin is incorporated as in **35** with a stability constant of $4 \cdot 10^7$ M^{-1} by apparently cooperative multitopic coordination. The host emission is quenched by this incorporation without emission from the central guest.

As a chelating ligand, 8-hydroxyquinoline (oxine) is interesting, since quenching-free metal ions such as Al^{3+} and Ga^{3+} are known to give very stable octahedral complexes. Therefore, the *meso*-oxinyl-appended porphyrin was synthesized and its *fac*-tris(oxinylporphynyl) gallium complex **36** was obtained. In the complex, three porphyrins are arranged like a pinwheel. The center-to-center distances between two porphyrin units a-b, b-c, and c-a in Figure 23 were 15, 17, and 18.5 Å, respectively.[90,91] The fluorescence intensity was increased in the coordination complex compared with the free porphyrin. The fluorescence anisotropy decay analyzed the energy transfer rate between three porphyrin components as ca. 10 ps. Considering the fluorescence lifetime of 8.6 ns, the energy is stored in the trisporphyrin complex that allows an energy transfer 800 times to neighboring porphyrins in its excited lifetime. The introduction of two oxinyl groups at the facing *meso*-positions extends the coordination organization further to a dendritic structure **37**. Even in such a large assembly, the fluorescence intensity was larger than that of the starting free porphyrin.

As a quenching-free external metal ion, Zn^{2+} may also be used for chelation organization. For this class of porphyrin assembly, Groves synthesized mono- and bisphenanthrolinyl-porphyrins, **38** and **39**, respectively.[92] Addition of the Zn^{2+} ion to **38** induced a red shift of the Soret band by head-to-tail interaction of porphyrins of orthogonal orientation (Figure 24). For the case of **39**, a larger shift and

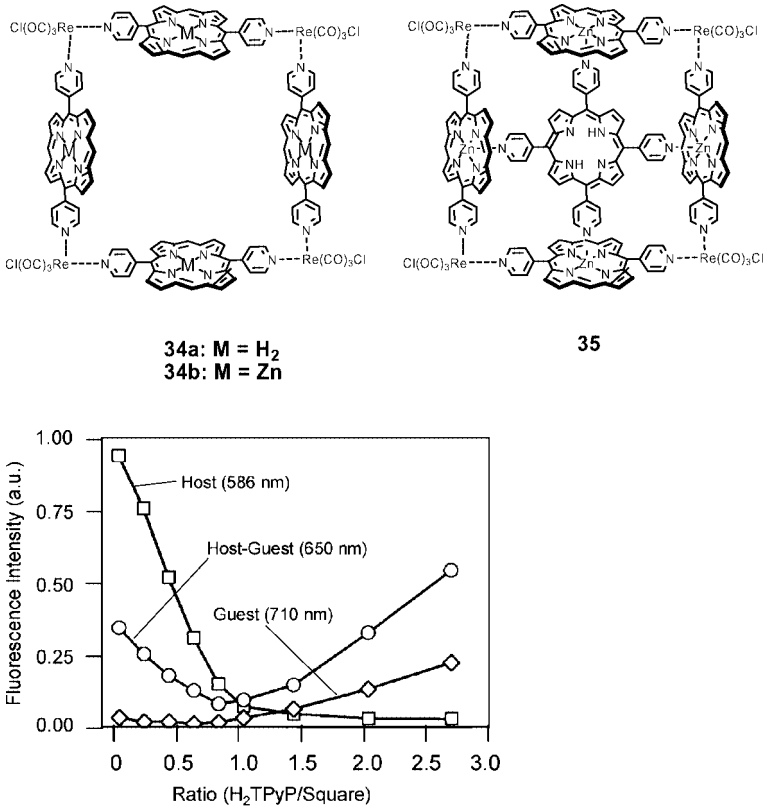

Figure 22. Fluorescence emission change on guest complexation into Re^{2+}-organized porphyrin square.[89]

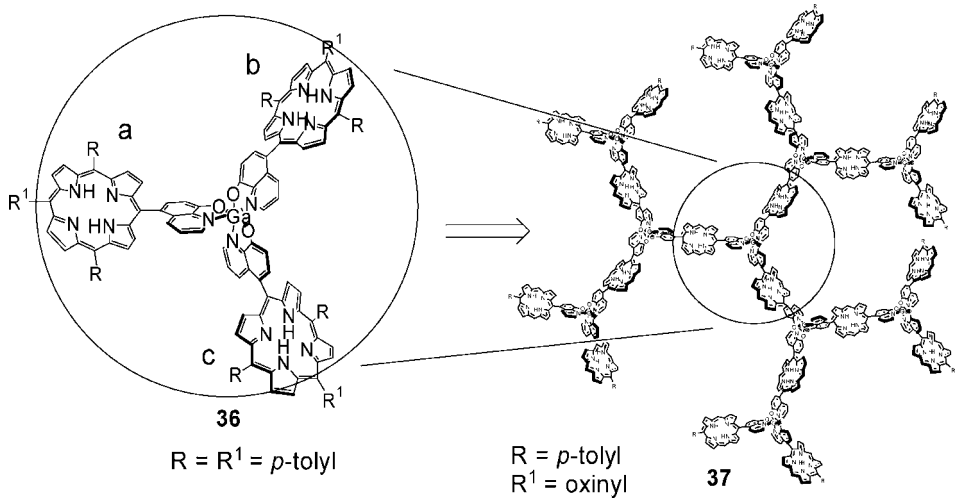

Figure 23. Ga^{3+}-organized oxinylzincporphyrin pinwheel and its dendritic growth.[90,91]

broadening of the Soret band were observed to show the development of exciton interaction. The average chain length of oligomer **40** was estimated from the complexation rate constant and estimated as 12.3 ± 0.5. The oligomeric products are potentially fluorescent.

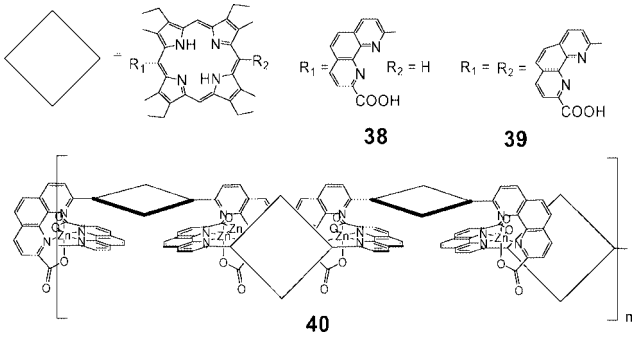

Figure 24. Mono- and bis(phenanthrolinyl)porphyrins and their Zn^{2+} complexation.[92]

The use of a flat electrode surface instead of a porous semiconductor one for a dye-sensitized solar cell may provide an interesting possibility. The problems arising from the decreased surface area must, however, be overcome. Gold nanoparticles have attracted wide interest in view of physical properties that are different from bulk materials. Nano-sized particles should have large surface areas that can be modified by appropriate functionalities. The surface can be modified and protected by alkanethiolate. Therefore, an ω-porphyrin-bearing alkanethiolate with or without simple alkanethiolate was employed to modify the gold nanoparticles so as to afford **41** and **42** (Figure 25).[93]

The fluorescence of porphyrin gold particles **41** and **42** showed a double exponential decay. The lifetime of the parent compound (9.5 ns in THF) was perturbed to contain short major components 0.15 ns (86%) and 0.17 ns (97%), for **41** and **42**, respectively. The average lifetimes are therefore calculated as 1.4 ns for **41** and 0.41 ns for **42**. This means that the fluorescence of the porphyrin is significantly quenched even on the surface of gold nanoparticles. However, the degree of quenching is smaller compared with the case in which the same porphyrin is modified on a two-dimensional Au(111) surface, the latter fluorescence lifetime being 0.04 ns. A fewer number of gold atoms on the 3D surface of nanoparticles compared with the planar Au(111) electrode surface is involved in energy transfer quenching. The decay rate ($7.7 \cdot 10^9$ s^{-1}) of the absorption at 460 nm agreed with the rise of the excited plasmon band at about 600 nm. This means that any electron-transfer system faster than 130 ps can compete favorably with this energy transfer quenching.[94–96]

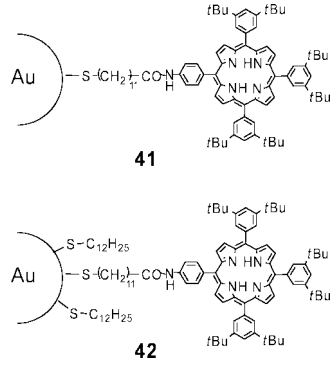

Figure 25. Porphyrin grafting on gold nanoparticle.[93]

The gold nanoparticles coated with a porphyrin-alkanethiolate **43** monolayer as in **44** were then treated with fullerene. Broad absorption appeared in the 700–800 nm region as a sign of a charge-transfer absorption band due to the π-complex formation between porphyrin and C_{60}. At the same time, these nanoparticles (**45**) were clusterized in solution as shown in **46** (Figure 26) and deposited on a SnO_2 electrode. The photocurrent action spectrum shows that the IPCE value increases with high concentrations of C_{60} and reaches ca. 30% at 490 nm. The excited singlet state porphyrin is quenched efficiently by C_{60} via electron transfer in the porphyrin-C_{60} complex rather than energy transfer to gold nanoparticles.

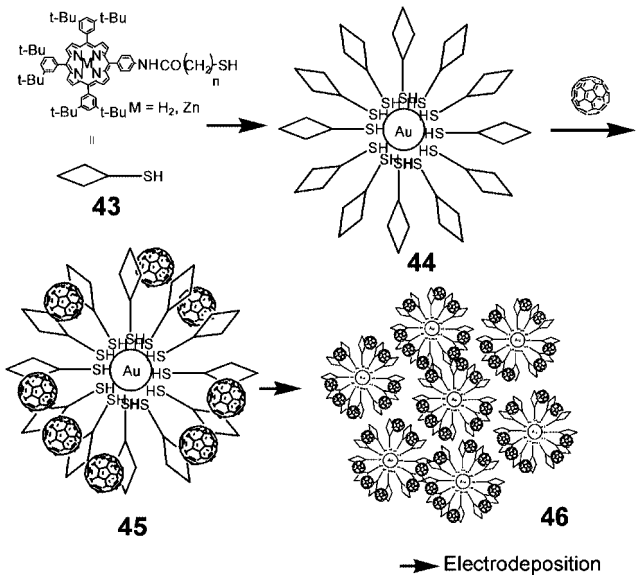

Figure 26. High order organization of porphyrin and fullerene with gold nanoparticles.[96]

The photoinduced charge separation is facilitated in the supramolecular complex of the porphyrin and C_{60}. The reduced C_{60} injects the electron into the conduction band of SnO_2 nanocrystallites, or the electron is relayed through hopping among the C_{60} molecules in the cluster. On the other hand, the oxidized porphyrin is regenerated by electron-transfer reduction with iodide in the electrolyte.[97]

7. Phthalocyanine

Compared with porphyrins, phthalocyanines have higher extinction coefficients in the Q-band region at longer wavelengths and emit fluorescence with much higher quantum yields. The metal-assisted organization of phthalocyanine in the past resulted in most cases in the quenching of singlet excitation energy. The author has been interested in incorporating phthalocyanine into supramolecular systems by using metal coordination. The first example is the use of the strategy of complementary coordination of an imidazolyl-zinc-porphyrin. Here the phthalocyanine unit is connected to the porphyrin as the *meso*-substituent. Two phthalocyanines are then connected through a complementary porphyrin dimer as **47**.[98] The absorption spectrum is a sum of two chromophores and covers a wide range of the visible region, just like the natural chlorophyll chromophores, but with an even larger extinction coefficient as illustrated in Figure 27. Excitation of any absorption range of porphyrin and phthalocyanine falls into the S_1(Q) state of phthalocyanine via efficient energy transfer to the lowest excited state. The fluorescence quantum yield from this state is as high as 0.71. Overall, the supermolecule is regarded as an excellent antenna composite having broad and strong absorption bands of both S_2 of porphyrin and S_1 of phthalocyanine and with a high fluorescence quantum yield from the lowest excited state of phthalocyanine.

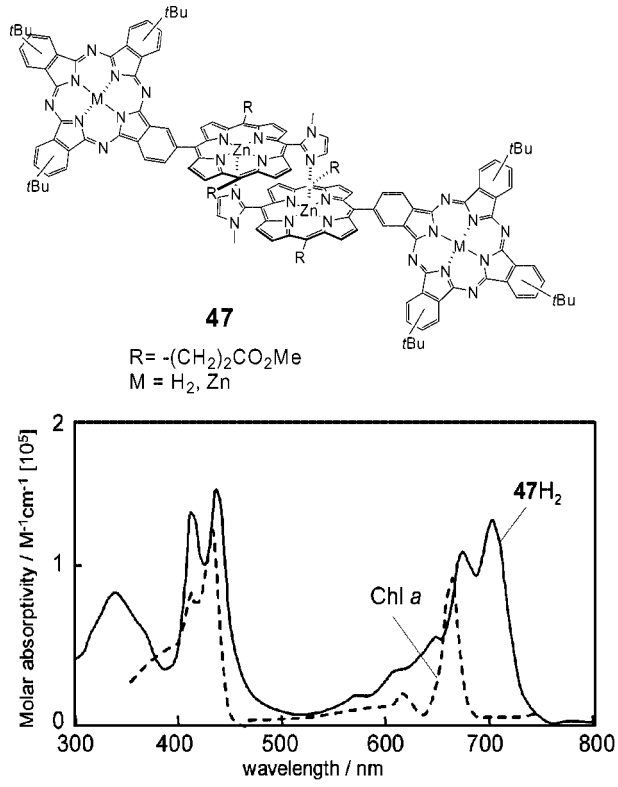

Figure 27. Complementary dimer formation of imidazolylzincporphyrin with phthalocyanine and comparison of the absorption spectrum with that of chlorophyll *a*.[98]

The above method is interesting in that phthalocyanines are brought into a highly fluorescent supermolecule. At the same time, it is challenging to develop a methodology to organize phthalocyanines themselves. Applying the same methodology as for porphyrins, an imidazolyl substituent was introduced at one of the benzo-groups of metallophthalocyanine.[99] A very stable dimer **48** (Figure 28) was formed with use of Zn^{2+} or Mg^{2+}-phthalocyanine, as observed by NMR, UV/visible and mass spectra. The Q-bands split by exciton interaction in the dimer converge into a single band on titrating with *N*-methylimidazole through a clear isosbestic point. That a large excess of competitive ligand was required to cleave the coordination bond reflects the large stability constant. The values were evaluated as large as $1.4 \cdot 10^{11}$–$1.1 \cdot 10^{12}$ M^{-1} for Zn^{2+}- and Mg^{2+}-phthalocyanines. The interaction of complementary coordination of imidazolyl-to-Zn^{2+} or Mg^{2+} was confirmed by characteristic higher-field shifts of the imidazolyl and the half of the ring protons that face each other to the large π-electronic system of phthalocyanine. The fluorescence of this dimer is not quenched on this assembly formation. The fluorescence quantum yields of the dimers from Zn(*t*Bu)$_3$, Zn(OBu)$_6$, and Mg(*t*Bu)$_3$-phthalocyanines were 0.26, 0.45, and 0.76, respectively. These values were almost identical to those of the starting monomeric species. The coordination organization of imidazolyl-porphyrin has thus been introduced into the field of phthalocyanine. A new version of supramolecular chemistry in the field of phthalocyanine will be interesting.

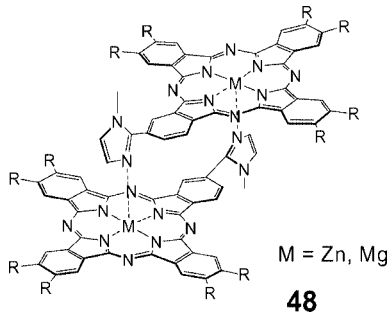

Figure 28. Complementary coordination of imidazolyl-M-(Zn,Mg)$^{2+}$-phthalocyanine.[99]

8. Perylenebisimide

As briefly overviewed in the general characteristics of chromophores, perylenebisimide shows excellent properties in light absorption and emission. The high aggregation tendency through the overlap of planar π-orbitals can be reduced when bulky substituents such as tetraaryloxy groups are introduced at the 1, 6, 7, and 12-positions.[100–104] According to the coordination organization proposed by Fujita, linear ligands were prepared most easily by introducing ligands at the imide nitrogen atoms of perylenebisimide. Then M(dppp), where dppp represents 1,3-bis(diphenylphosphanyl)propane, afforded in quantitative yields macrocyclotetramers **49** of perylenebisimides appended with various aryloxy groups with use of M = Pt^{2+} and Pd^{2+} (Figure 29).[105] These complexes remain intact at concentrations as low as ca. 10^{-6} M. Even if transition-metal ions are used in this case, the fluorescence quantum yield of the starting perylenebisimide in the square remained largely intact at a level of nearly 90%.

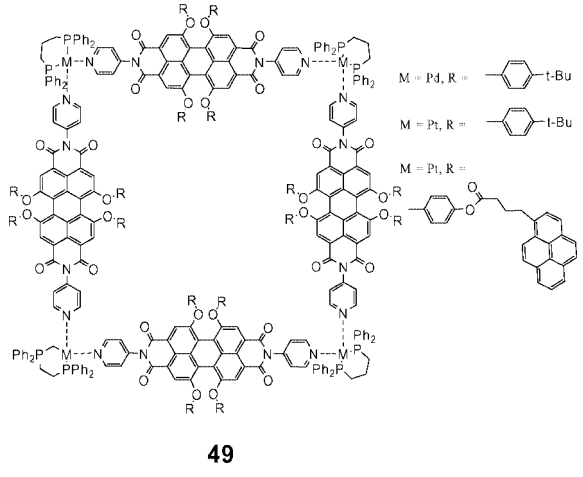

Figure 29. Macrocyclo-tetramerization of pyridyl-appended tetraaryloxyperylenebisimide by Pd^{2+} or Pt^{2+} complex.[105]

When pyrene is introduced at the 1, 6, 7, and 12 positions as the aryloxy substituent, the square has a large number of chromophores, 16 pyrene and four perylenebisimide chromophores, appropriate for light harvesting to cover a wide range of wavelengths with high molar extinction coefficients. Photophysical measurements were undertaken by steady state and time-resolved emission and transient absorption spectroscopy. Compared with the simple phenyl-substituted square, efficient (90%) and fast (0.2 ns) energy transfer from the pyrene to the perylenebisimide chromophores quenched almost completely the pyrenyl fluorescence. At the same time, very fast and efficient (>94%) electron transfer from pyrene to perylene reduced significantly the fluorescence from the perylene.

When bis(terpyridyl)-functionalized perylenebisimide **50** was subjected to self-assembly by metal coordination, linear metallo-supramolecular polymers (**51**) could be obtained (Figure 30).[106–109] Isothermal titration calorimetry studies of the terpyrydine ligand with various transition-metal ions established that Zn^{2+} afforded a very stable bis(terpyridyl) complex with the successive stability constants $K_1 > 10^8$ M^{-1} and $K_2 > 10^{10}$ M^{-1}, demonstrating a clear tendency for stable 2:1 complex formation. The complexes exhibited intense red fluorescence (λ_{max} = 620 nm) with the quantum yield of ca. 0.9. The complexation with Zn^{2+} has virtually no effect on the fluorescence quantum yield, although the use of Fe^{2+} for the assembly formation induces a quenching down to $\Phi_{fl} < 0.1$. Likewise, fluorescence lifetimes of Zn^{2+} dimer and polymer complexes were the same as that of the uncomplexed ligand, showing no electronic interaction between $Zn(tpy)_2$ and perylene sites. The complex showed reversibility of the binding event within a short timescale less than 1 min.

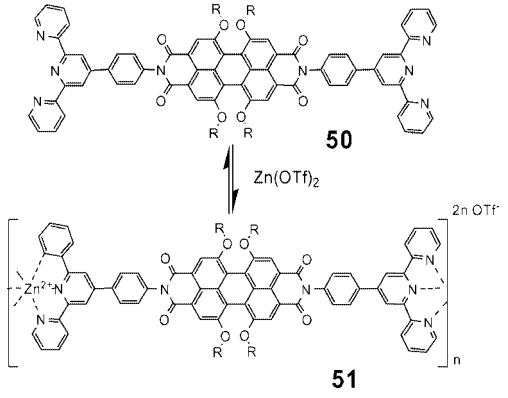

Figure 30. Bis(tpy)-connected polymerization of tetraaryloxyperylenebisimide.[106]

The process was monitored by fluorescence anisotropy titration. When fluorescence anisotropy r is plotted as a function of the Zn^{II}/perylene monomer ratio, the r value increased almost linearly to a maximum of r = 0.133 at a 1:1 ratio of Zn^{2+}/**50**. The observations are compatible with the reversibility of the assembly formation, since the anisotropy decay due to the rotational diffusion of polymer must be slower. In the linear rigid coordination polymer, the transition-dipole moments align along the N–N axis of the perylenebisimide unit, and energy transfer within the perylenebisimide units along the same polymeric chain will not induce the anisotropy decrease. After 1:1 stoichiometry, a fragmentation process leading to the oligomeric units occurs and the anisotropy tends to decrease again, but never reaches the value of the monomer unit.

The dynamic character of ligand exchange was tested in solution by mixing two different perylenebisimide ligands **I** and **II** in a 1:1 molar ratio.[110] These ligands have the same molecular length and differ only in their alkyl groups at the phenoxy substituents. ^{1}H and ^{31}P NMR spectra after the equilibrium suggested the formation of an ideal statistical mixture. Mass spectra proved the existence of all the molecular squares **A**, **B**, **C**, **D**, **E**, and **F** (Figure 31) in the resulting solution.

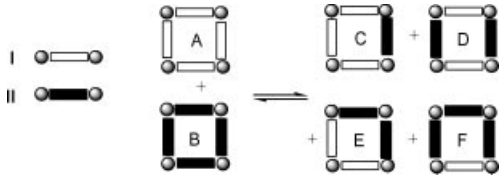

Figure 31. Ligand exchange equilibrium after mixing two molecular squares.[110]

9. Polypyridyl Metal Complexes

Bipyridyl (bpy), terpyridyl (tpy), phenanthrolyl (phen) metal complexes belong to this class and afford stable complexes with various metal ions. The ruthenium tris(bpy) complex and its derivatives play important roles on dye-sensitized solar cells.

The emission quantum yield from $^{3}MLCT$ of $Ru(bpy)_3$ is relatively high at 0.04, but $[Ru(tpy)_2]^{2+}$ emits with a low quantum yield of $1\cdot10^{-5}$ with a lifetime of 250 ps. The terpyridine complex is characterized by a directed connection and its large stability constant. When two tpy units are connected through a *m*-phenylene group its complexation with Ru^{2+} ion affords automatically a macrocyclic hexamer of the $[Ru(tpy)_2]^{2+}$ complex **52** (Figure 32).[111] When carbazole is substituted as the central connecting unit, pentameric macrocycles are self-assembled by complexation with Zn^{2+}, Ru^{2+}, and Fe^{2+} ions (**53**).[112] Although carbazole itself is highly fluorescent, the pentamacrocyclic Ru^{2+} complex does not show fluorescence at all. On the other hand, the Zn^{2+} macrocycle shows a strong emission at 560 nm. The macropentacyclic $[M(tpy)_2]^{2+}$ complexes were used for coating of nanocrystalline TiO_2 in a Grätzel-type solar cell device. The Ru^{2+} complex gave the highest photoconversion efficiency (η) of the cell, η being 1.53, 0.73, and 0.49% for the Ru^{2+}, Zn^{2+}. and Fe^{2+} cases, respectively.

The $[Ru(tpy)_2]^{2+}$ complex is suitable for connecting other chromophores in a linear fashion. When $Ru(tpy)_2$ connects porphyrins as in **54**, the energy absorbed by the porphyrin is transferred to the lowest triplet state with 100% efficiency (Figure 33).[113] Triplet energy transfer from $^{3}PAu\text{-}Ru\text{-}PH_2$ to $PAu\text{-}Ru\text{-}^{3}PH_2$ with a center-to-center separation of 21 Å was examined. The energy transfer was mediated by the interposed Ru complex by an exchange mechanism at 77 K with a rate constant of $2.5\cdot10^{7}\ s^{-1}$, which is as fast as the arylene-connected case.

Hanan reports that the lifetime of $^{3}MLCT$ emission from $[Ru(tpy)_2]^{2+}$ increases significantly by the introduction of

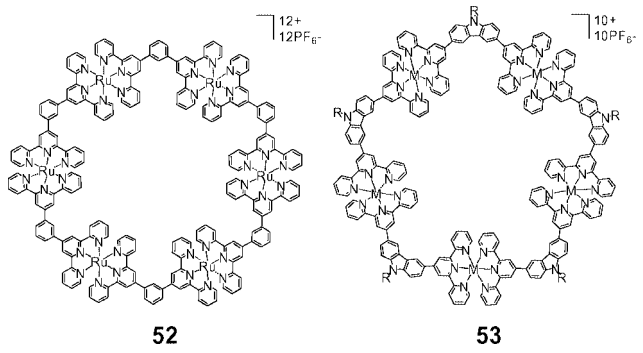

Figure 32. Macrohexamer and pentamer of $[Ru(tpy)_2]^{2+}$.[111,112]

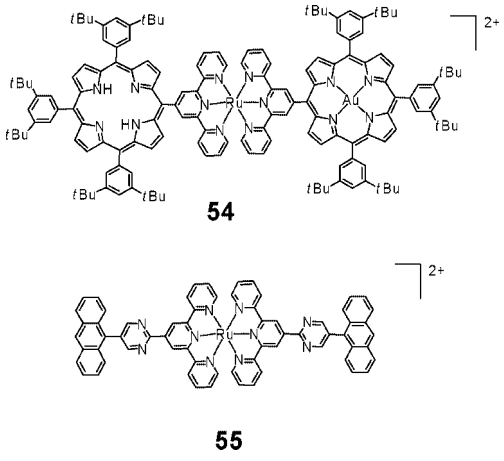

Figure 33. Connection of porphyrins through $[Ru(tpy)_2]^{2+}$ complex and $[Ru^{2+}(anthracenyl\text{-}tpy)_2]^{2+}$ complex.[113,114]

an anthracene moiety as in **55**.[114] The luminescence decay lasts up to 1.8 μs at room temperature. The phenomenon is explained by the equilibrium between the initially formed $^{3}MLCT$ state of $[Ru(tpy)_2]^{2+}$ and the low-lying anthracene-based triplet states. Introduction of organic chromophores having triplet excited states of energies close to the $^{3}MLCT$ is claimed to be an efficient way to prolong the short excited-state lifetime of the $[Ru(tpy)_2]^{2+}$.

The dendritic Ru(biscarbazolyl-phenanthroline)$_3$ complex **56** shows a red shift of absorption and emission maxima compared to $Ru(phen)(bpy)_2$ **57** (Figure 34).[115] The excitation spectrum resembles the absorption spectrum and

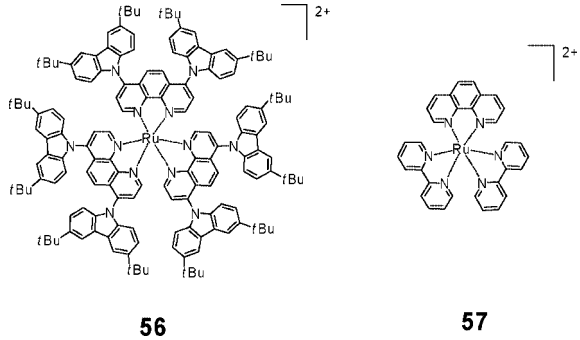

Figure 34. Ru(biscarbazolyl-phenanthroline)$_3$ and $Ru(phen)(bpy)_2$ complexes.[115]

the fluorescence from the carbazolyl part is completely quenched. These properties suggest its potential usefulness for the antenna function.

10. Conclusion and Outlook

The research on light-harvesting antenna has been much inspired by very aesthetic X-ray crystallographic structures of antenna complexes of the photosynthetic purple bacteria. The energy degeneracy of each component in the ring structure is important for transferring the energy efficiently to targets in any direction. Many chromophores having large extinction coefficients in the visible wavelength region have been organized into macrocyclic structures. New supramolecular methodologies have been developed and have succeeded in providing macrocycles of not only 2D but also 3D arrangements. Photophysical studies have elucidated the rate of the fast excitation energy hopping process by anisotropy decay after polarized light excitation and also by exciton-exciton annihilation. In the development of artificial antenna complexes, noncyclic systems are important too. Linear arrays without loss of excitation energy have also been developed. In order to obtain stable supramolecular complexes, transition-metal ions have been frequently used. In most cases, intersystem crossing leads to the triplet state. The analysis of such systems becomes difficult in most cases and awaits further photophysical studies.

Acknowledgments

We thank our collaborators and co-workers, whose work is reported in this article. This work has been supported by Grants-in-Aid for Scientific Research (A) (No. 15205020) and Scientific Research on Priority Areas (No. 15036248), Reaction Control of Dynamic Complexes from the Ministry of Education, Culture, Sports, Science, and Technology of the Japanese Government.

[1] A. K. Burrell, D. L. Officer, P. G. Plieger, D. C. W. Reid, *Chem. Rev.* **2001**, *101*, 2751–2796.
[2] D. Holten, D. F. Bocian, J. S. Lindsey, *Acc. Chem. Res.* **2002**, *35*, 57–69.
[3] D. Kim, A. Osuka, *Acc. Chem. Res.* **2004**, *37*, 735–745.
[4] M.-S. Choi, T. Yamazaki, I. Yamazaki, T. Aida, *Angew. Chem. Int. Ed.* **2004**, *43*, 150–158.
[5] H. Imahori, *J. Phys. Chem. B* **2004**, *108*, 6130–6143.
[6] J. C. Chambron, V. Heitz, J.-P. Sauvage in *The Porphyrin Handbook* (Eds.: K. M. Kadish, K. M. Smith, R. Guilard), Academic Press, New York, **1999**, vol. 6, chapter 40, pp. 1–42.
[7] S. Takagi, H. Inoue in *Molecular and Supramolecular Photochemistry* (Eds.: V. Ramamurthy, K. S. Schanze), Marcel Decker, New York, **1999**, vol. 4, chapter 6, pp. 251–342.
[8] J. K. M. Sanders in *The Porphyrin Handbook* (Eds.: K. M. Kadish, K. M. Smith, R. Guilard), Academic Press, New York, **2000**, vol. 3, pp. 347–368.
[9] M. Tabata, J. Nishimoto in *The Porphyrin Handbook* (Eds.: K. M. Kadish, K. M. Smith, R. Guilard), Academic Press, New York, **2000**, vol. 9, pp. 221–419.
[10] J. Wojaczynski, L. Latos-Grazynski, *Coord. Chem. Rev.* **2000**, *204*, 113–171.
[11] E. Iengo, E. Zangrando, E. Alessio, *Eur. J. Inorg. Chem.* **2003**, 2371–2384.
[12] P. D. Harvey in *The Porphyrin Handbook* (Eds.: K. M. Kadish, K. M. Smith, R. Guilard), Academic Press, New York, **2003**, vol. 18, pp. 63–249.
[13] K. Ogawa, Y. Kobuke in *Encyclopedia of Nanoscience and Nanotechnology* (Ed.: H. S. Nalwa), American Scientific Publishers, Stevenson Ranch, California, **2003**, vol. 10, 1–30.
[14] T. S. Balaban, "Light-Harvesting Nanostructures", in *Encyclopedia of Nanoscience and Nanotechnology* (Ed.: H. S. Nalwa), American Scientific Publishers, Stevenson Ranch, CA, **2004**, vol. 4, pp. 505–559.
[15] A. Satake, Y. Kobuke, *Tetrahedron* **2005**, *61*, 13–41.
[16] Y. Kobuke, *Structure and Bonding*, in press.
[17] S. Karrasch, P. A. Bullough, R. Ghosh, *EMBO J.* **1995**, *14*, 631–638.
[18] G. McDermott, S. M. Prince, A. A. Freer, A. M. Hawthornthwaite-Lawless, M. Z. Papiz, R. J. Cogdell, N. W. Isaacs, *Nature* **1995**, *374*, 517–521.
[19] M. Z. Papiz, S. M. Prince, T. Howard, R. J. Cogdell, N. W. Isaacs, *J. Mol. Biol.* **2003**, *326*, 1523–1538.
[20] R. J. Cogdell, N. W. Isaacs, A. A. Freer, T. D. Howard, A. T. Gardiner, S. M. Prince, M. Z. Pappiz, *FEBS Lett.* **2003**, *555*, 35–39.
[21] S. Bahatyrova, R. N. Frese, C. A. Siebert, J. D. Olsen, K. O. van der Werf, R. Van Grondelle, R. A. Niederman, P. A. Bullough, C. Otto, C. N. Hunter, *Nature* **2004**, *430*, 1058–1062.
[22] X. Hu, A. Damjanovic, T. Ritz, K. Schulten, *Proc. Natl. Acad. Sci. USA* **1998**, *95*, 5935–5941.
[23] A. P. Shreve, J. K. Trautman, H. A. Frank, T. G. Owens, A. C. Albrecht, *Biochim. Biophys. Acta* **1991**, *1058*, 280–288.
[24] R. Jimenez, S. N. Dikshit, S. E. Bradforth, G. R. Fleming, *J. Phys. Chem.* **1996**, *100*, 6825–6834.
[25] L. M. P. Beekman, F. van Mourik, M. R. Jones, H. M. Visser, C. N. Hunter, R. van Grondelle, *Biochem.* **1994**, *33*, 3143–3147.
[26] S. Hess, M. Chachisvilis, K. Timpmann, M. R. Jones, C. N. Hunter, V. Sundström, *Proc. Natl. Acad. Sci. USA* **1995**, *92*, 12333–12337.
[27] X. Hu, T. Ritz, A. Damjanovic, K. Schulten, *J. Phys. Chem. B* **1997**, *101*, 3854–3871.
[28] C. Jungas, J.-L. Ranck, J.-L. Rigaud, P. Joliot, A. Vermeglio, *EMBO J.* **1999**, *18*, 534–542.
[29] A. W. Roszak, T. D. Haward, J. Southall, A. T. Gardiner, C. J. Law, N. W. Isaacs, R. J. Cogdell, *Science* **2003**, *302*, 1969–1972.
[30] S. Scheuring, F. Francia, J. Busselez, B. A. Melandri, J.-L. Rigaud, D. Levy, *J. Biol. Chem.* **2004**, *279*, 3620–3626.
[31] P. Jordan, P. Fromme, H. T. Witt, O. Klukas, W. Saenger, N. Krauss, *Nature* **2001**, *411*, 909–917.
[32] B. R. Green, W. W. Parson (Eds.), "Light-Harvesting Antennas", in *Advances in Photosynthesis and Respiration* (Ed.: Govindjee), vol. 13, Kluwer Academic Publishers, **2003**.
[33] Z. Liu, H. Yan, K. Wang, T. Kuang, J. Zhang, L. Gui, X. An, W. Chang, *Nature* **2004**, *428*, 287–292.
[34] N. Nelson, A. Ben-Shem, *Bioessays* **2005**, *27*, 914–922.
[35] D. L. Andrews (Ed.), *Energy Harvesting Materials*, World Scientific, Hackensack, NJ, **2005**.
[36] M. A. Palacios, F. L. de Weerd, J. A. Ihalainen, R. van Grondelle, H. V. Amerongen, *J. Phys. Chem. B* **2002**, *106*, 5782–5787.
[37] G. Weber, F. W. J. Teale, *Faraday Trans.* **1957**, *53*, 646–655.
[38] T. P. Causgrove, P. Cheng, D. C. Brune, R. E. Blankenship, *J. Phys. Chem.* **1993**, *97*, 5519–5524.
[39] D. J. Quimby, F. R. Longo, *J. Am. Chem. Soc.* **1975**, *97*, 5111–5117.
[40] K. Kamioka, R. A. Cormier, T. W. Lutton, J. S. Connolly, *J. Am. Chem. Soc.* **1992**, *114*, 4414–4415.
[41] D. Kim, J. Terner, T. G. Spiro, *J. Am. Chem. Soc.* **1986**, *108*, 2097–2099.
[42] J. S. Lindsey, J. N. Woodford, *Inorg. Chem.* **1995**, *34*, 1063–1069.
[43] P. G. Seybold, M. Gouterman, *J. Mol. Spectrosc.* **1969**, *31*, 1–13.

[44] R. O. Loutfy, E. R. Menzel, *J. Am. Chem. Soc.* **1980**, *102*, 4967–4970.
[45] D. F. O'Shea, M. A. Miller, H. Matsueda, J. S. Lindsey, *Inorg. Chem.* **1996**, *35*, 7325–7338.
[46] R. Dobrawa, M. Lysetska, P. Ballester, M. Grüne, F. Würthner, *Macromolecules* **2005**, *38*, 1315–1325.
[47] L. J. Henderson Jr, F. R. Fronczek, W. R. Cherry, *J. Am. Chem. Soc.* **1984**, *106*, 5876–5879.
[48] M. Maestri, N. Armaroli, V. Balzani, E. C. Constable, A. M. W. C. Thompson, *Inorg. Chem.* **1995**, *34*, 2759–2767.
[49] G. Ferraudi in *Phthalocyanines, Properties and Applications* (Eds.: C. C. Leznoff, A. B. P. Lever), Wiley-VCH, New York, **1989**, vol. 1, chapter 4, pp. 291–340.
[50] H. Du, R. A. Fuh, J. Li, A. Corkan, J. S. Lindsey, *Photochem. Photobiol.* **1998**, *68*, 141–142.
[51] M. Kasha, H. R. Rawls, M. A. El-Bayyoumi, *Pure Appl. Chem.* **1965**, *11*, 371–392.
[52] Y. Kobuke, K. Ogawa, *Bull. Chem. Soc. Jpn.* **2003**, *76*, 689–708.
[53] Y. Kobuke, *J. Porphyrins Phthalocyanines* **2004**, *8*, 156–174.
[54] Y. Kobuke, H. Miyaji, *J. Am. Chem. Soc.* **1994**, *116*, 4111–4112.
[55] Y. Kobuke, H. Miyaji, *Bull. Chem. Soc. Jpn.* **1996**, *69*, 3563–3569.
[56] K. Ogawa, Y. Kobuke, *Angew. Chem. Int. Ed.* **2000**, *39*, 4070–4073.
[57] D. Furutsu, A. Satake, Y. Kobuke, *Inorg. Chem.* **2005**, *44*, 4460–4462.
[58] A. Nomoto, Y. Kobuke, *Chem. Commun.* **2002**, 1104–1105.
[59] A. Nomoto, H. Mitsuoka, H. Ozeki, Y. Kobuke, *Chem. Commun.* **2003**, 1074–1075.
[60] A. Ohashi, A. Satake, Y. Kobuke, *Bull. Chem. Soc. Jpn.* **2004**; *77*, 365–374.
[61] T. M. Trnka, R. H. Grubbs, *Acc. Chem. Res.* **2001**, *34*, 18–29.
[62] M. Morisue, S. Yamatsu, N. Haruta, Y. Kobuke, *Chem. Eur. J.* **2005**, *11*, 5563–5574.
[63] R. Takahashi, Y. Kobuke, *J. Am. Chem. Soc.* **2003**, *125*, 2372–2373.
[64] R. Takahashi, Y. Kobuke, *J. Org. Chem.* **2005**, *70*, 2745–2753.
[65] I.-W. Hwang, D. M. Ko, T. K. Ahn, D. Kim, F. Ito, Y. Ishibashi, S. R. Khan, Y. Nagasawa, H. Miyasaka, C. Ikeda, R. Takahashi, K. Ogawa, A. Satake, Y. Kobuke, *Chem. Eur. J.* **2005**, *11*, 3753–3761.
[66] Y. Kuramochi, A. Satake, Y. Kobuke, *J. Am. Chem. Soc.* **2004**, *126*, 8668–8669.
[67] C. Ikeda, N. Nagahara, N. Yoshioka, H. Inoue, *New J. Chem.* **2000**, *24*, 897–902.
[68] C. Ikeda, Y. Tanaka, T. Fujihara, Y. Ishii, T. Ushiyama, K. Yamamoto, N. Yoshioka, H. Inoue, *Inorg. Chem.* **2001**, *40*, 3395–3405.
[69] A. Tsuda, S. Sakamoto, K. Yamaguchi, T. Aida, *J. Am. Chem. Soc.* **2003**, *125*, 15722–15723.
[70] T. S. Balaban, R. Goddard, M. Linke-Schaetzel, J.-M. Lehn, *J. Am. Chem. Soc.* **2003**, *125*, 4233–4239.
[71] P. Ballester, A. Costa, P. M. Deya, A. Frontera, R. M. Gomila, A. I. Oliva, J. K. M. Sanders, C. A. Hunter, *J. Org. Chem.* **2005**, *70*, 6616–6622.
[72] R. A. Haycock, A. Yartsev, U. Michelsen, V. Sundström, C. A. Hunter, *Angew. Chem. Int. Ed.* **2000**, *39*, 3616–3619.
[73] E. Iengo, E. Zangrando, E. Alessio, J.-C. Chambron, V. Heitz, L. Flamigni, J.-P. Sauvage, *Chem. Eur. J.* **2003**, *9*, 5879–5887.
[74] S. Anderson, H. L. Anderson, A. Bashall, M. AcParlin, J. K. M. Sanders, *Angew. Chem. Int. Ed. Engl.* **1995**, *34*, 1096–1099.
[75] S. Rucareanu, O. Mongin, A. Schuwey, N. Hoyler, A. Gossauer, W. Amrein, H.-U. Hediger, *J. Org. Chem.* **2001**, *66*, 4973–4988.
[76] I.-W. Hwang, H. S. Cho, D. H. Jeong, D. Kim, A. Tsuda, T. Nakamura, A. Osuka, *J. Phys. Chem. B* **2003**, *107*, 9977–9988.
[77] A. Tsuda, T. Nakamura, S. Sakamoto, K. Yamaguchi, A. Osuka, *Angew. Chem. Int. Ed.* **2002**, *41*, 2817–2821.
[78] I.-W. Hwang, T. Kamada, T. K. Ahn, D. M. Ko, T. Nakamura, A. Tsuda, A. Osuka, D. Kim, *J. Am. Chem. Soc.* **2004**, *126*, 16187–16198.
[79] A. Tsuda, H. Hu, R. Tanaka, T. Aida, *Angew. Chem. Int. Ed.* **2005**, *44*, 4884–4888.
[80] A. Prodi, M. T. Indelli, C. J. Kleverlaan, F. Scandola, E. Alessio, T. Gianferrara, L. G. Marzilli, *Chem. Eur. J.* **1999**, *5*, 2668–2679.
[81] A. Prodi, C. Chiorboli, F. Scandola, E. Iengo, E. Alessio, R. Dobrawa, F. Würthner, *J. Am. Chem. Soc.* **2005**, *127*, 1454–1462.
[82] M. Fujita, J. Yazaki, K. Ogura, *J. Am. Chem. Soc.* **1990**, *112*, 5645–5647.
[83] M. Fujita, K. Ogura, *Bull. Chem. Soc. Jpn.* **1996**, *69*, 1471–1482.
[84] M. Fujita, *Chem. Soc. Rev.* **1998**, *27*, 417–425.
[85] M. Fujita, *Acc. Chem. Res.* **1999**, *32*, 53–61.
[86] A. Prodi, C. J. Kleverlaan, M. T. Indelli, F. Scandola, E. Alessio, E. Iengo, *Inorg. Chem.* **2001**, *40*, 3498–3504.
[87] C. M. Drain, F. Nifiatis, A. Vasenko, J. D. Batteas, *Angew. Chem. Int. Ed.* **1998**, *37*, 2344–2347.
[88] T. Milic, J. C. Garno, J. D. Batteas, G. Smeureanu, C. M. Drain, *Langmuir* **2004**, *20*, 3974–3983.
[89] R. V. Slone, J. T. Hupp, *Inorg. Chem.* **1997**, *36*, 5422–5423.
[90] I. V. Rubtsov, Y. Kobuke, H. Miyaji, K. Yoshihara, *Chem. Phys. Lett.* **1999**, *308*, 323–328.
[91] Y. Kobuke, H. Miyaji, K. Ogawa, *J. Supramol. Chem.* **2002**, *14*, 159–170.
[92] K. P. McNaughton, J. T. Groves, *Org. Lett.* **2003**, *5*, 1829–1832.
[93] H. Imahori, M. Arimura, T. Hanada, Y. Nishimura, I. Yamazaki, Y. Sakata, S. Fukuzumi, *J. Am. Chem. Soc.* **2001**, *123*, 335–336.
[94] T. Hasobe, H. Imahori, P. V. Kamat, S. Fukuzumi, *J. Am. Chem. Soc.* **2003**, *125*, 14962–14963.
[95] H. Imahori, Y. Kashiwagi, Y. Endo, T. Hanada, Y. Nishimura, I. Yamazaki, Y. Araki, O. Ito, S. Fukuzumi, *Langmuir* **2004**, *20*, 73–81.
[96] T. Hasobe, H. Imahori, P. V. Kamat, T. K. Ahn, S. K. Kim, D. Kim, A. Fujimoto, T. Hirakawa, S. Fukuzumi, *J. Am. Chem. Soc.* **2005**, *127*, 1216–1228.
[97] H. Imahori, A. Fujimoto, S. Kang, H. Hotta, K. Yoshida, T. Umeyama, Y. Matano, S. Isoda, M. Isosomppi, N. V. Tkachenko, H. Lemmetyinen, *Chem. Eur. J.* **2005**, *11*, 7265–7275.
[98] K. Kameyama, A. Satake, Y. Kobuke, *Tetrahedron Lett.* **2004**, *45*, 7617–7620.
[99] K. Kameyama, M. Morisue, A. Satake, Y. Kobuke, *Angew. Chem. Int. Ed.* **2005**, *44*, 2–5.
[100] G. Seybold, C. Wagenblast, *Dyes Pigm.* **1989**, *71*, 303–317.
[101] R. Gvishi, R. Reisfeld, Z. Burshtein, *Chem. Phys. Lett.* **1993**, *213*, 338–344.
[102] D. Dotcheva, M. Klapper, K. Mullen, *Macromol. Chem. Phys.* **1994**, *195*, 1905–1911.
[103] F. Würthner, C. Thalacker, A. Sautter, *Adv. Mater.* **1999**, *11*, 754–758.
[104] F. Würthner, C. Thalacker, A. Sautter, *Angew. Chem. Int. Ed.* **2000**, *39*, 1243–1245.
[105] C.-C. You, F. Würthner, *J. Am. Chem. Soc.* **2003**, *125*, 9716–9725.
[106] R. Dobrawa, F. Würthner, *Chem. Commun.* **2002**, 1878–1879.
[107] F. Würthner, *Chem. Commun.* **2004**, 1564–1579.
[108] R. Dobrawa, M. Lysetska, P. Ballester, M. Grüe, F. Würthner, *Macromolecules* **2005**, *38*, 1315–1325.
[109] R. Dobrawa, F. Würthner, *J. Polymer Sci. A Polymer Chem.* **2005**, *43*, 4981–4995.
[110] F. Würthner, A. Sautter, D. Schmid, P. J. A. Weber, *Chem. Eur. J.* **2001**, *7*, 894–902.
[111] G. R. Newkome, T. J. Cho, C. N. Moorefield, G. R. Baker, R. Cush, P. S. Russo, *Angew. Chem. Int. Ed.* **1999**, *38*, 3717–3721.

[112] S.-H. Hwang, P. Wang, C. N. Moorefield, L. A. Godínez, J. Manríquez, E. Bustosc, G. R. Newkome, *Chem. Commun.* **2005**, 4672–4674.
[113] L. Flamigni, F. Barigelletti, N. Armaroli, B. Ventura, J.-P. Collin, J.-P. Sauvage, J. A. G. Williams, *Inorg. Chem.* **1999**, *38*, 661–667.
[114] R. Passalacqua, F. Loiseau, S. Campagna, Y.-Q. Fang, G. S. Hanan, *Angew. Chem. Int. Ed.* **2003**, *42*, 1608–1611.
[115] N. D. McClenaghan, R. Passalacqua, F. Loiseau, S. Campagna, B. Verheyde, A. Hameurlaine, W. Dehaen, *J. Am. Chem. Soc.* **2003**, *125*, 5356–5365.

Received: February 23, 2006
Published Online: May 17, 2006

